Hindawi
International Journal of Antennas and Propagation
Volume 2020, Article ID 6209081, 7 pages
https://doi.org/10.1155/2020/6209081

Research Article

A Balun Bandpass Filter to Facilitate the Design of Dual-Polarized Dipole Antenna

He Huang

Key Laboratory of Equipment Efficiency in Extreme Environment, Ministry of Education, School of Aerospace Science and Technology, Xidian University, Xi'an 710071, China

Correspondence should be addressed to He Huang; huanghe@xidian.edu.cn

Received 17 July 2020; Revised 12 October 2020; Accepted 25 October 2020; Published 5 November 2020

Academic Editor: Muhammad Ramlee Kamarudin

A dipole antenna based on a balun bandpass filter (BPF) is developed in this paper. The balun BPF employs two U-shaped resonators settled on the left side of the open-circuited transmission line and two L-shaped stubs to produce signals with equal amplitude and inverse phase. In this way, the volume of the balun BPF is reduced by half, and the distance between two output ports is dramatically decreased. Then, the balun BPF is integrated with a dipole. Instead of the traditional Γ-shaped line with a wide balun ground, two thin microstrip lines with width of 1 mm are adopted to connect the dipole and the balun BPF. The antenna bandwidth is further extended due to the fusion of the resonance of the dipole and balun BPF. As a result, the proposed antenna can operate from 4350 to 5025 MHz (covering the n79 band of 5G NR, 4400 MHz–5000 MHz), yielding a good filtering performance in the stopband. The measured half-power beamwidth is ranging from 61° to 63° and the measured gain is ranging from 7.95 to 8.5 dBi in the passband. This new balun BPF and the dual-polarized dipole based on it have great potential to be applied in 5G MIMO systems.

1. Introduction

In many radio frequency wireless systems, the bandpass filter (BPF) has been widely used. In [1], two back-to-back broadband microstrip-to-CPW transitions are employed to form a wide passband at the center frequency of 6.85 GHz. In [2], a dual-mode dual-band BPF with four transmission zeros which uses a microstrip-to-slotline balun structure is proposed.

In the meantime, the balun BPF, which can not only provide response suppression but also transfer the unbalanced single-ended signal into balanced differential signals, is developed. In a few years, dual-mode balun BPF based on the ring resonator [3], square-loop resonator [4], cross slot patch resonator [5], and a loop resonator with Y-type stub embedded [6] would have been gradually proposed. Other type of balun BPFs such as [7, 8] have also been investigated. In [7], by providing two coupling paths through microstrip and coplanar-waveguide, good amplitude and phase imbalances in the two passbands are achieved. Balun BPF using coupled lines with capacitive loads are discussed in [8]. Slight amplitude variation and phase imbalance is obtained. New approach based on the open-circuited half-wave transmission line has been proposed afterwards [9–12]. The odd- and even-mode analysis method is used to analyze it. However, the comparative large distance of the output ports of these antennas make it difficult to integrate with antennas.

In the meanwhile, several approaches that directly integrate the balun BPF with the antenna have been discussed. In [13], a third-order filtering microstrip antenna array is presented. Its feeding network owns the function of the filter, thus preserving a good selectivity at band edges. The design in [14] is based on the filter composed of coupled open-loop resonators. Finally, the CP patch antenna exhibits good out-of-band rejection over a wide band. The device in [15] employs a four-way out-of-phase resonator, coupling the energy from the slots to the patches and rendering a filtering response at S-band. In [16], a differential filtering patch antenna excited by a balun BPF is developed. The patch is printed on the top side and two slots are etched on the

middle layer. Finally, a filtering antenna operating at 2.45 GHz is obtained. All the antennas involved in [13–16] are patch type, and all of them are using the coupled lines with capacitive loads to implement the bandpass filter.

In this paper, a balun bandpass filter for dual-polarized dipole antennas application has been explored. The working mechanism of the balun BPF is similar to the ones in [9–12], but it occupies smaller volume and smaller distance between output ports. This balun BPF is elaborately designed so that its two output ports are very close while maintaining the equal amplitude and antiphase output. These two advantages make the balun BPF easy to assemble with the dipole and further realize dual polarization. A dual-polarized antenna based on such filtering power divider which could operate from 4350 MHz to 5025 MHz is finally fabricated and investigated. It has a good frequency selectivity at the band edge. The proposed antenna could be very promising to weaken the interference between the different antennas in 5G systems.

2. Design of the Balun BPF

Figure 1 shows the configuration of the balun BPF. It is made of a substrate which has a dielectric constant of 2.65, a loss tangent of 0.02, and a thickness of 0.8 mm. On the top layer of the substrate, there are open-circuited transmission lines, two U-shaped coupling structures, and a pair of L-shaped stubs with balanced ports. The ground is on the bottom layer of the substrate.

The length of the open-circuited transmission line (*L_feed*) is about 0.52 λ_g (λ_g is the guided wavelength at 4.85 GHz). On the left side of the microstrip line, two U-shaped coupling structures are settled back-to-back. The simple U-shaped structure is chosen because the target bandwidth is not very wide. The length of the U-shaped structure ($l1 + l2 + l3$) is chosen as half-wave length at the center point of the operating band. Note that the opening of the upper U-shaped structure should face downwards, and the opening of the lower U-shaped structure should face upwards, thus guaranteeing the surface current is opposite with respect to the reference point as Figure 2 indicates. A pair of L-shaped microstrip lines is placed nearby the U-shaped resonators to couple the energy to the balanced ports while not changing the inverse characteristics of the current on the U-shaped structure. As seen from Figure 2, the vector current on the end of the upper L-shaped stub is flowing out from Port 1, while the one on the end of the lower L-shaped stub is flowing into Port 2. The out-of-phase signal is thus obtained.

Figure 3(a) gives the S-parameters of the proposed balun BPF. The balun BPF operates from 4750 MHz to 5000 MHz when the return loss is larger than 14 dB (VSWR >1.5). At the same time, a wide stopband is obtained. The insertion losses for Ports 1 and 2 are, respectively, −3.3 dB and −3.4 dB. Figure 3(b) gives the amplitude and phase differences of output Ports 1 and 2. It shows that the amplitude imbalance is within 0.45 dB and phase difference is about $180^\circ \pm 2^\circ$ over the passband.

To further illustrate the working mechanism of the balun BPF, some key parameters such as the total length of the U-shaped resonator ($l1 + l2 + l3$), the length of the open-circuited transmission line (*L_feed*), the gap between the open-circuited line and the U-shaped resonator (*g1*), the gap between the L-shaped stub and the U-shaped resonator (*g2*), and the distance between the two L-shaped stubs (*g3*) are studied. The simulated process is conducted using the commercial electromagnetic simulation software HFSS. Figure 4(a) shows how the value of $l1 + l2 + l3$ affects the $|S_{33}|$ curves. As it increases with a step of 0.15 mm, the central frequency point is shifted to the lower band. The variation regularity of *L_feed* is similar to it, and the description of which is not repeated here. Figure 4(b) shows the effect of *g1* on the reflection coefficient of the balun BPF. It is found that *g1* affects not only the resonant frequency but also the impedance matching degree of the balun BPF. That is to say, *g1* determines the amount and intensity of the energy coupled from the open circuited transmission line to the U-shaped resonator. The variation regularity of *g2* is similar to the one of *g1*, and duplicate discussion will be omitted. Figure 4(c) plots the $|S_{33}|$ curves in allusion to the change of *g3*. With the increase of *g3*, the effective length of the open-circuited transmission line is equivalently increased, making the resonant point shift down. After optimizing the parameters, the final dimensions are determined as follows (unit: millimeter): $W\_feed = 1.5$, $L\_feed = 20.2$, $l1 = 9.75$, $l2 = 4.4$, $l3 = 9.75$, $l4 = 9.75$, $l5 = 5$, $g1 = 0.25$, $g2 = 0.2$, and $g3 = 0.7$.

3. Dipole Antenna Integrated with the Balun BPF

With the design scheme mentioned above, the size of the balun BPF is reduced by half compared with the ones in [9–11]. Besides, the distance between the two output ports is dramatically decreased compared with ones in [3–16]. These two advantages make the balun BPF suitable to integrate with the dipole antenna and further to constitute the dual-polarized radiation. Since the output signal of the balun BPF has been transformed into balanced signal with equal amplitude and antiphase, the traditional Γ-shaped line with a wide balun ground is no longer needed. Instead, two thin microstrip lines with width of only 1 mm are adopted to connect the dipole and the balun BPF, as shown in Figures 5 and 6. Another benefit of this design is that the antenna bandwidth can be further extended due to the resonance merged between the dipole and balun BPF.

To verify the feasibility of the design, a dual-polarized dipole antenna assembled with the balun BPF is fabricated and measured. Its photograph is shown in Figure 7. The S-parameters curves are depicted in Figure 8. It shows that the resonance of the balun BPF at 4.8 GHz is merged with the dipole's resonance point at 4.4 GHz, thus providing a bandwith of 14% from 4350 to 5025 MHz. Port isolation over the working band is larger than 35 dB, which benefits from

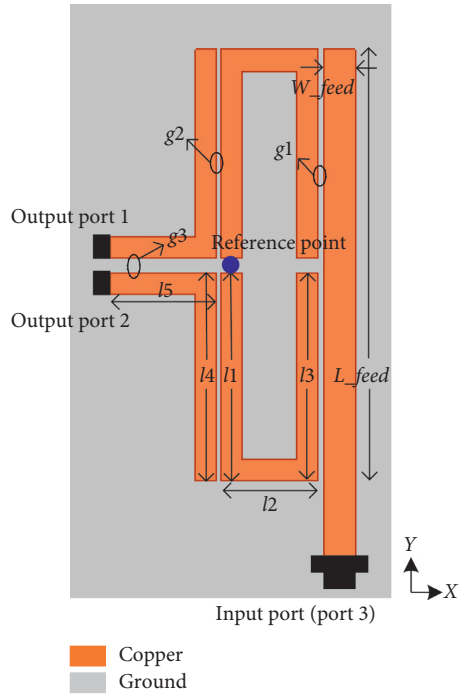

Figure 1: Geometry of the balun BPF.

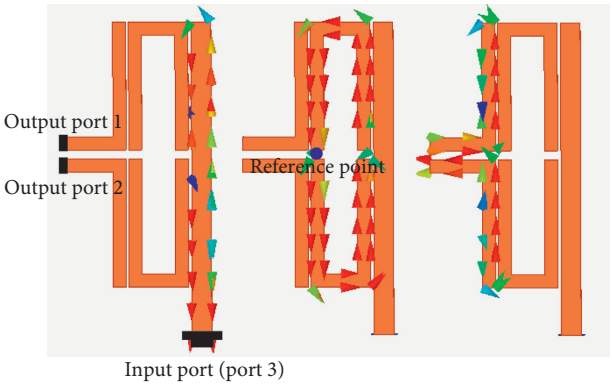

Figure 2: Vector current distribution on the open-circuited transmission line, U-shaped coupling structure, and L-shaped stub at a certain phase.

the vertical polarization of the two dipoles. A wide stop band can also be observed.

The simulated and measured H-plane pattern at 4.4 GHz, 4.7 GHz, and 5 GHz is given in Figure 9 (when Port 3a is excited). The simulated and measured half-power beamwidth (HPBW) is around 60° and 62°, and the minimum cross polarization discrimination is 18.6 dB and 21.2 dB. The simulated in-band gain is ranging from 8.3 to 8.7 dBi and the measured one is from 7.95 to 8.5 dBi, as shown in Figure 10. The results reveal that the antenna could provide unidirectional radiation and good frequency selectivity in the entire band.

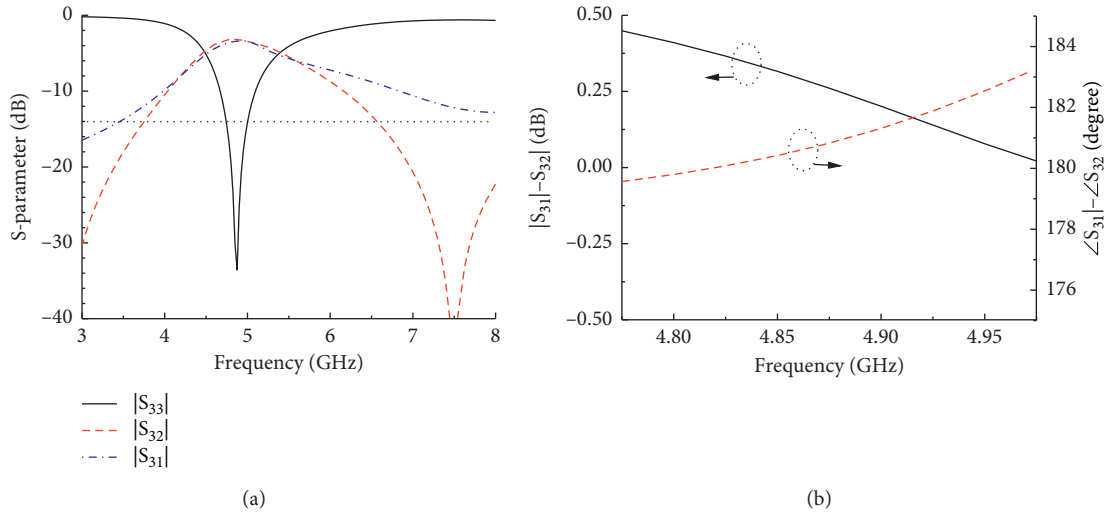

Figure 3: (a) S-parameters of the balun BPF. (b) Amplitude imbalance and phase difference.

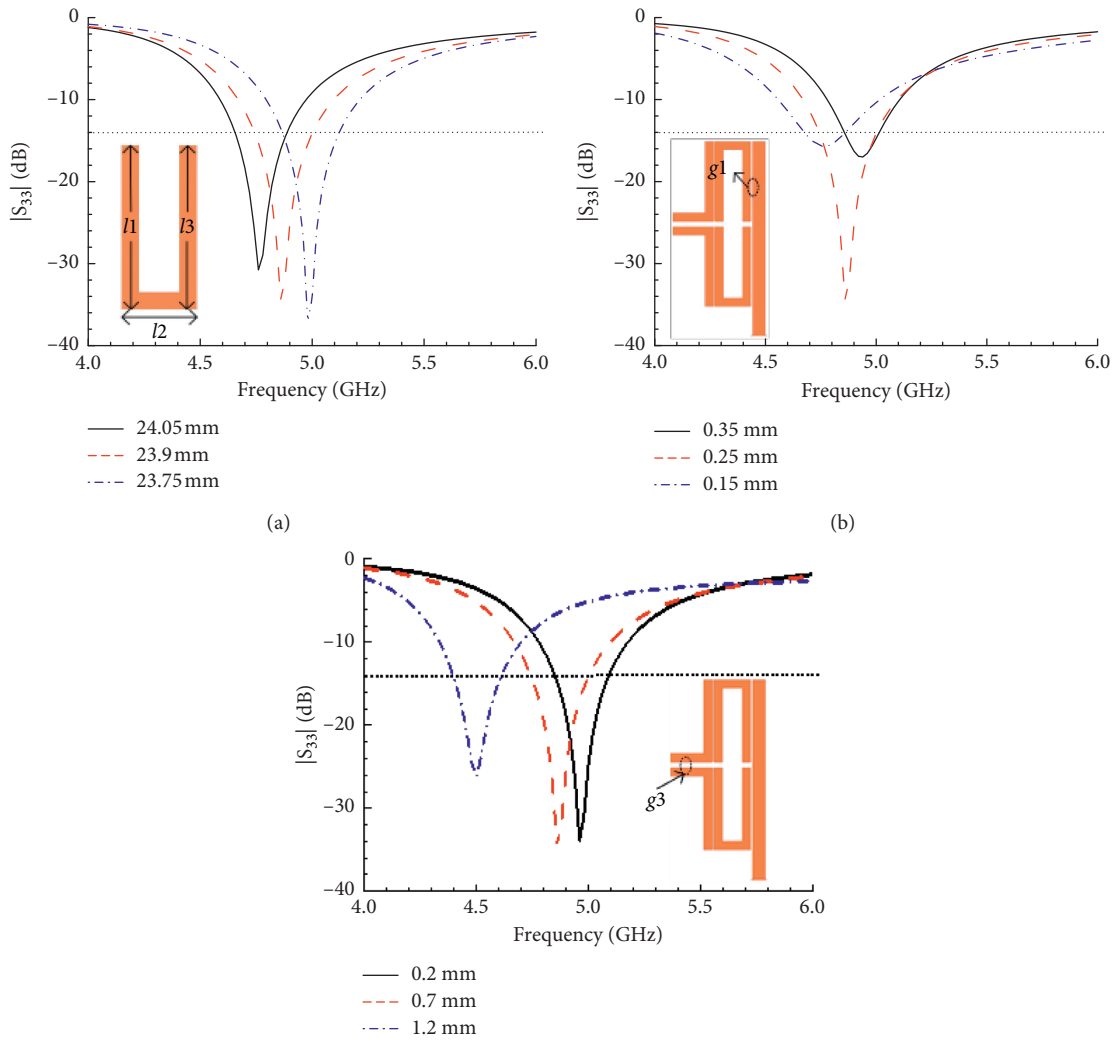

Figure 4: (a) Effects of $l1 + l2 + l3$ on $|S_{33}|$. (b) Effects of $g1$ on $|S_{33}|$. (c) Effects of $g3$ on $|S_{33}|$.

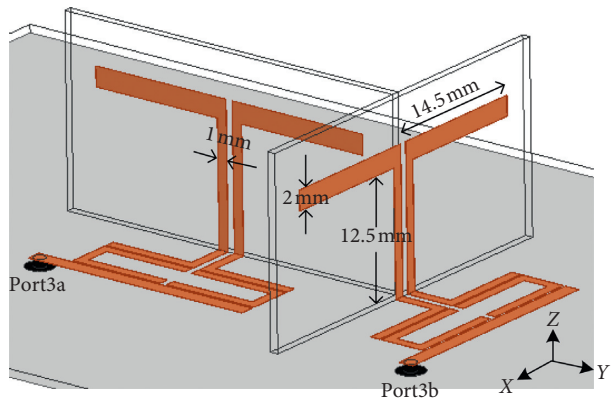

Figure 5: Configuration of the dipole antenna which is assembled with the balun BPF.

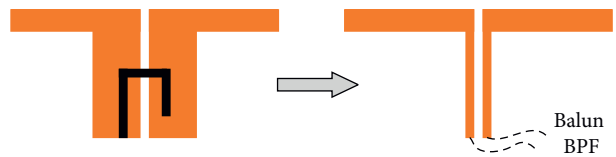

Figure 6: The dipoles fed by traditional balun or by a novel balun BPF.

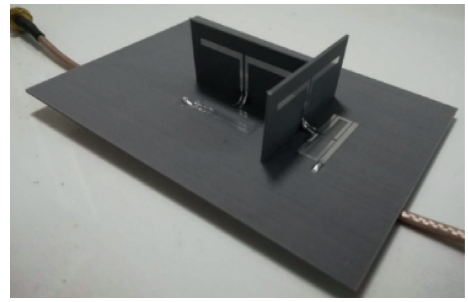

Figure 7: Photograph of the proposed antenna.

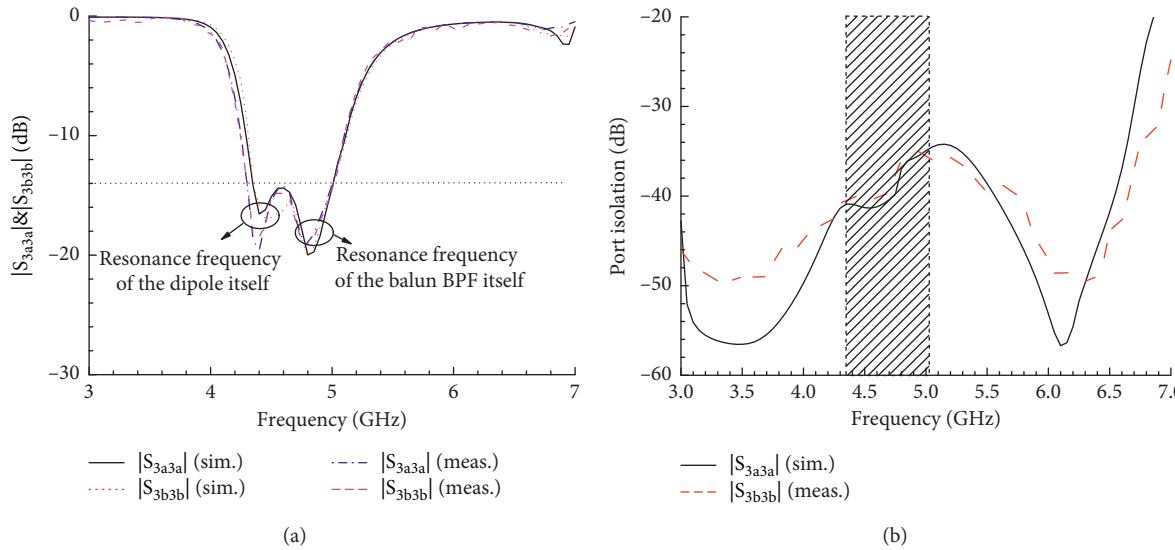

Figure 8: (a) Simulated and measured $|S_{3a3a}|$ and $|S_{3b3b}|$ of the antenna. (b) Simulated and measured port isolation of the antenna.

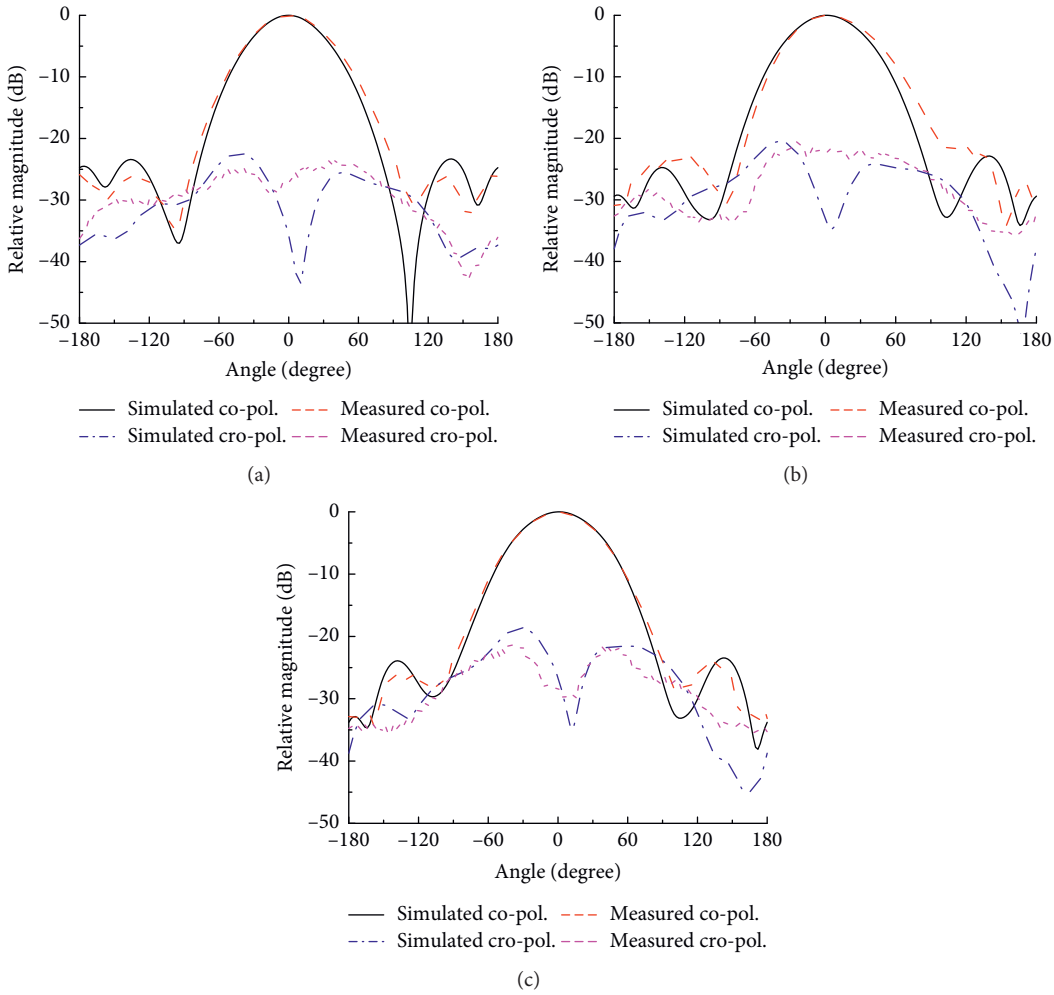

Figure 9: Simulated and measured H-plane pattern at 4.4 GHz, 4.7 GHz, and 5 GHz.

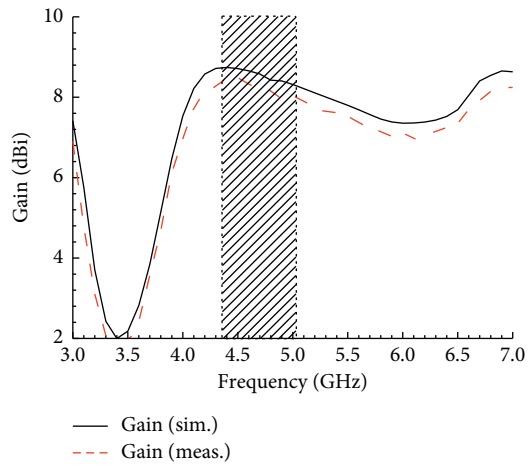

Figure 10: Simulated and measured gain over the entire band.

4. Conclusion

When antennas with different working frequencies are placed in the same space, they can sense each other's energy. Even though their respective S-parameters appear to be normal, it cannot work effectively and false alarms occur. To solve the problem, the BPF is connected to the antennas to suppress the unwanted signals.

In this paper, a filtering power divider resonating at around 4.85 GHz is designed. It makes use of the out-of-phase feature of the standing wave distribution along the open-circuited transmission line, designing a single mode power divider with high frequency selectivity. Different from the ones in [9–12], the proposed balun BPF employs two U-shaped resonators settled on one side of the open-circuited transmission line. Two L-shaped stubs for coupling the energy is placed nearby the U-shaped resonators. The volume of the balun BPF is reduced by half, and the distance between two output ports is greatly decreased. Results show that the power divider exhibits a great filtering performance in the stopband and excellent balance performance with 0.45 dB amplitude imbalance and 2° phase imbalance.

Then, the balun BPF is directly integrated with a dipole. The traditional Γ-shaped feedline with a wide balun ground is replaced by two very thin lines for connection. Furthermore, due to the fusion of the resonance of the dipole and balun BPF, the antenna bandwidth could be further extended.

As a result, the proposed antenna can work from 4350 to 5025 MHz (covering the n79 band of 5G NR), yielding a good filtering performance in the stopband. Stable HPBW and high gain in the pass band is obtained. This new balun BPF and the dipole antenna based on it could be very promising in 5G MIMO systems.

Data Availability

The data used to support the findings of this study are included within the article.

Conflicts of Interest

The authors declare that they have no conflicts of interest.

Acknowledgments

The authors wish to acknowledge the support from the National Natural Science Foundation of China under Grants 61901321 and 61627901.

References

[1] J.-W. Baik, T.-H. Lee, and Y.-S. Kim, "UWB bandpass filter using microstrip-to-CPW transition with broadband balun," *IEEE Microwave and Wireless Components Letters*, vol. 17, no. 12, pp. 846–848, 2007.

[2] J.-W. Baik, L. Zhu, and Y.-S. Kim, "Dual-mode dual-band bandpass filter using balun structure for single substrate configuration," *IEEE Microwave and Wireless Components Letters*, vol. 20, no. 11, pp. 613–615, 2010.

[3] S.-J. Kang and H.-Y. Hwang, "Ring-balun-bandpass filter with harmonic suppression," *IET Microwaves, Antennas & Propagation*, vol. 4, no. 11, pp. 1847–1854, 2010.

[4] P. Cheong, T.-S. Lv, W.-W. Choi, and K.-W. Tam, "A compact microstrip square-loop dual-mode balun-bandpass filter with simultaneous spurious response suppression and differential performance improvement," *IEEE Microwave and Wireless Components Letters*, vol. 21, no. 2, pp. 77–79, 2011.

[5] S. Sun and W. Menzel, "Novel dual-mode balun bandpass filters using single cross-slotted patch resonator," *IEEE Microwave and Wireless Components Letters*, vol. 21, no. 8, pp. 415–417, 2011.

[6] S. S. Gao and S. Sun, "Compact dual-mode balun bandpass filter with improved upper stopband performance," *Electronics Letters*, vol. 47, no. 23, pp. 1281–1283, 2011.

[7] G.-S. Huang and C. H. Chen, "Dual-band balun bandpass filter with hybrid structure," *IEEE Microwave and Wireless Components Letters*, vol. 21, no. 7, pp. 356–358, 2011.

[8] C. Tan, H. Wang, G. Yang, and J.-Z. Zhao, "A balun-BPF using coupled lines with capacitive loads," in *Proceedings of the International Conference on Computational Problem-Solving (ICCP)*, pp. 73–75, Leshan, China, December 2012.

[9] C. Cai, J. Wang, L. Zhu, and W. Wu, "A new approach to design microstrip wideband balun bandpass filter," *IEEE Microwave and Wireless Components Letters*, vol. 26, no. 2, pp. 116–118, 2016.

[10] H. Xu, J. Wang, L. Zhu, F. Huang, and W. Wu, "Design of a dual-mode balun bandpass filter with high selectivity," *IEEE Microwave and Wireless Components Letters*, vol. 28, no. 1, pp. 22–24, 2018.

[11] P. Kim, Qi Wang, G. Chaudhary, and Y. Jeong, "A design of balun bandpass filter for wide stopband Attenuation base on stepped impedance resonators," in *Proceedings of the Asia-Pacific Microwave Conference*, pp. 1339–1341, Kyoto, Japan, November 2018.

[12] J. Wang, F. Huang, L. Zhu, C. Cai, and W. Wu, "Study of a new planar-type balun topology for application in the design of balun bandpass filters," *IEEE Transactions on Microwave Theory and Techniques*, vol. 64, no. 9, pp. 2824–2832, 2016.

[13] C.-K. Lin and S.-J. Chung, "A filtering microstrip antenna array," *IEEE Transactions on Microwave Theory and Techniques*, vol. 59, no. 11, pp. 2856–2863, 2011.

[14] Z. H. Jiang, M. D. Gregory, and D. H. Werner, "Design and experimental investigation of a compact circularly polarized integrated filtering antenna for wearable biotelemetric devices," *IEEE Transactions on Biomedical Circuits and Systems*, vol. 10, no. 2, pp. 328–338, 2016.

[15] C.-X. Mao, S. Gao, Y. Wang et al., "An integrated filtering antenna array with high selectivity and harmonics suppression," *IEEE Transactions on Microwave Theory and Techniques*, vol. 64, no. 6, pp. 1798–1805, 2016.

[16] H. Jin, G. Q. Luo, K.-S. W. Che et al., "Vertically-integrated differential filtering patch antenna excited by a balun bandpass filter," *IET Microwaves, Antennas & Propagation*, vol. 13, no. 3, pp. 300–304, 2019.